Evaporation and deposition of alkyl-capped silicon nanocrystals in ultrahigh vacuum

Y. Chao, L. Šiller, S. Krishnamurthy, P. R. Coxon, U. Bangert, M. Gass, L. Kjeldgaard, S. N. Patole, L. H. Lie, N. O'Farrell, T. A. Alsop, A. Houlton and B. R. Horrocks*[1]

Supporting Information

Contents

1 Methods **2**

1.1 Preparation of alkyl-SiNCs 2

1.2 Etching of Single Crystal Hydrogen-terminated Silicon Wafers 2

1.3 Monolayer preparation 3

1.4 Evaporation and deposition of C_{11}-SiNCs in UHV 3

1.5 AFM and STM Imaging 4

1.6 Raman and Luminescence Microspectroscopy 5

1.7 Infrared Spectroscopy 5

2 Additional Supporting Data **5**

2.1 Optical Microscopy 5

2.2 Atomic force and scanning tunneling microscopy 6

2.3 Raman - Luminescence Microscopy 8

2.4 X-ray Diffraction (XRD) 11

2.5 Scanning transmission electron microscopy (STEM) 13

2.6 Small angle x-ray scattering - particle sizing 17

2.7 Infrared spectroscopy 18

[1] b.r.horrocks@ncl.ac.uk

1 Methods

1.1 Preparation of alkyl-SiNCs

The preparation of the alkylated silicon nanocrystals (C_{11}-SiNCs) used in this work has been discussed in more detail elsewhere;[1, 2] here we give a brief summary and indicate a small simplification in the previously reported technique. This procedure produces C_{11}-SiNCs with substantially the same optical characteristics as before.

First, photoluminescent porous silicon layers were formed by galvanostatic anodisation of p-Si(100) wafer (boron doped, 10 Ω cm resistivity, Compart Technology, Peterborough, UK) in a 1:1 v/v solution of 48% aqueous HF and ethanol solution. The electrochemical cell was machined from PTFE and circular in cross-section. The silicon wafer was sealed to the base using a Teflon-coated Viton^{TM} O-ring. The counter electrode was a piece of tungsten wire coiled into a loop to improve the uniformity of the current distribution and the etching was carried out using a constant current source made in-house. A layer of luminescent porous silicon was made at high current density (5 min at 500 mA cm^{-2}) and used directly for formation of C_{11}-SiNCs by reflux in undecene/toluene without cleaving the porous layer from the chip; this is the point at which the procedure differs from that previously reported.[1] The hydrogen-terminated chip was dried under vacuum on a grease-free vacuum line (employing Young's taps) and then transferred into a Schlenk flask in which the hydrosilation reaction to form C_{11}-SiNCs was performed. The porous silicon was refluxed for 4h in a dry toluene solution (Merck, distilled over Na) containing 1 mol dm^{-3} of the alkene (1-undecene, Merck) until a clear yellow liquid formed. A small number of experiments (small angle x-ray scattering) were carried out using C_6-SiNCs made with 1-hexene instead. Solvent and unreacted alkene was removed under reduced pressure with a rotary pump and the yellow powder of C_{11}-SiNCs that remained was re-dissolved by stirring in toluene or dichloromethane as required. Occasionally, an oily residue is formed which is due to polymerisation of the alkene and can be avoided by decreasing the time spent under reflux and coevaporation with dichloromethane.

1.2 Etching of Single Crystal Hydrogen-terminated Silicon Wafers

Single crystal Si samples were cut from <111> oriented wafers (1-20 Ω cm, <0.1 degrees miscut angle, phosphorus-doped & n-type; Compart Technology, Cambridge, UK) to a size of ca. 1 x 1 cm using a diamond pencil. These chips were degreased in boiling trichloroethylene for 20 min, followed by acetone for 5 min and isopropanol for 5 min, before being rinsed thoroughly with water. A clean oxide layer was then grown in freshly prepared pirhana solution (4:1 v/v concentrated H_2SO_4 and 30% H_2O_2) for 15 min at 80^{o}C. The chips were then removed, washed

thoroughly with water and transferred to a sealed Teflon etching cell containing semiconductor grade NH_4F (40% v/v in water) saturated with Ar. The chips were etched in the solution under an Ar atmosphere at an orientation of 45 degrees with the polished side facing downwards. The NH_4F etchant was degassed by purging with Ar for 1h prior to immersion of the chips. After removal from the etchant, the wafers were rinsed with water for a few seconds and dried by wicking at the edge with filter paper.

1.3 Monolayer preparation

The hydrogen-terminated silicon chips were transferred to a Schlenk flask containing ~3 mL undecene dissolved in dry mesitylene (5% v/v in undecene) and placed under dry N_2 on a vacuum line. The vacuum line was constructed with grease-free Young's taps and joints to avoid any possible contamination of the samples with vacuum grease. The reaction was refluxed for 3h after which the wafers were rinsed with dichloromethane, acetone and finally dried in a stream of N_2. This reaction produces a silicon surface covered with an organic monolayer that is anchored by Si-C bonds directly to the bulk semiconductor and can be stably imaged by both AFM and STM in air. We denote this surface Si(111)-C11.

1.4 Evaporation and deposition of C_{11}-SiNCs in UHV

A thick film of C_{11}-SiNCs (a waxy yellow solid, ca. 0.1 mg typical) was deposited from dichloromethane solution on a tantalum plate and, after evaporation of the solvent, was placed in the UHV chamber. The C_{11}-SiNCs on the tantalum plate are referred to as the source. The receiving substrate, e.g., a 1 x 1 cm piece of Si(111)-C11 wafer was positioned in the UHV chamber facing the source at a distance of about 10 cm (figure 1). The tantalum plate (source) was heated resistively and its temperature was monitored by a K-type thermocouple. The receiving substrate was either allowed to remain at ambient temperature (ca. 20^{o}C) or, in a few experiments, cooled to 77K by connection to a liquid N_2 cold finger, but ambient AFM images showed little difference. The chamber was evacuated and baked so that the base pressure was typically 5 x 10^{-10} Torr. When a stable base pressure had been obtained, the temperature of the source was raised to 200^{o}C for a controlled period of time (typically $\leq$30 min). The chamber pressure typically rose to ca. 1.0 x 10^{-8} Torr during heating and the residual gas in the chamber was found by mass spectrometry (Quadrex 200 residual gas analyser, mass range 0-200 amu, Leybold Inficon Inc.) to consist of H_2, H_2O and N_2/CO. No evidence of solvent or C11 hydrocarbons was observed during heating.

In situ photoemission experiments on evaporated C_{11}-SiNCs carried out at beamline I511 of MAX-Lab (Lund, Sweden) employed a similar configuration.

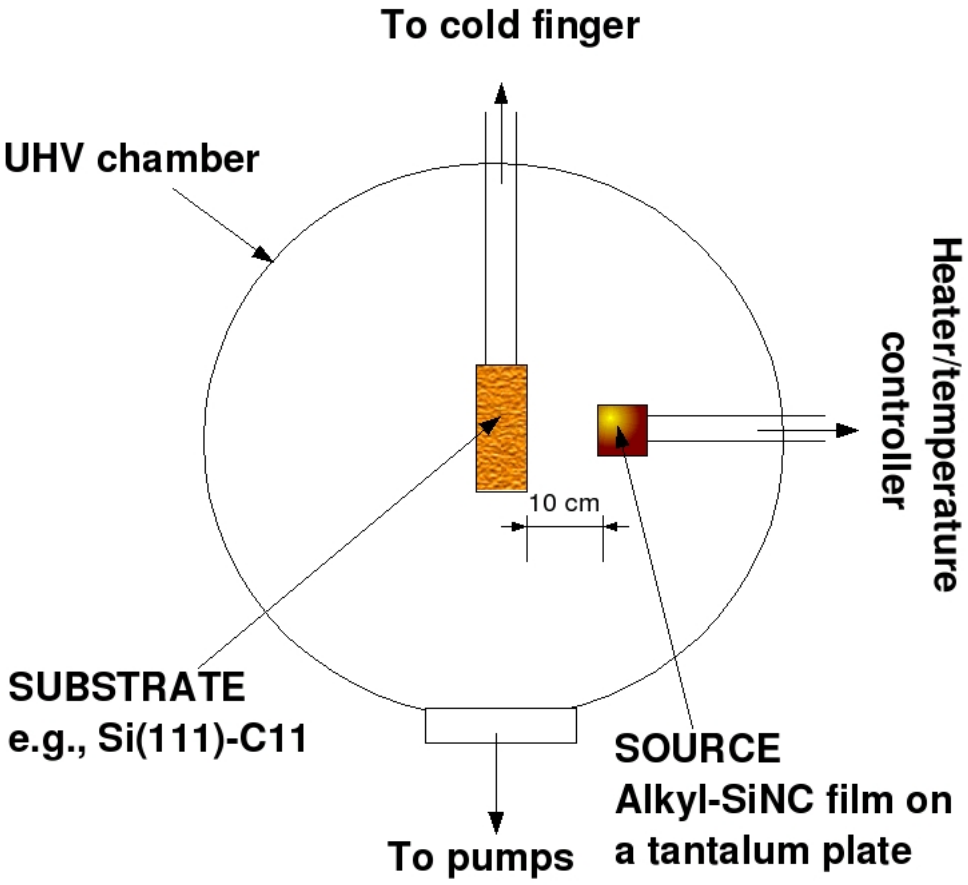

Figure 1: Schematic showing the experimental configuration for evaporation of C_{11}-SiNCs.

1.5 AFM and STM Imaging

The scanning probe microscope for both AFM and STM was a Nanoscope IIIa / Multimode system (Digital Instruments, Santa Barbara, CA) running the Nanoscope III version 5.12 r3 software. All reported AFM images were acquired in Tapping^{TM} mode. The cantilevers were ultrasharp noncontact silicon cantilevers supplied by MikroMasch (Spain) with a tip radius of curvature of 10 nm, cone angle of 20^o to 25^o and a force constant of about 40 N m^{-1}. The free resonance frequency of the cantilever was around 325 kHz. The drive amplitude was typically under 100 mV while the set point amplitude was kept between 1000 and 2000 mV. The scan rate was 1 Hz and the images contain 512 x 512 data points. All the images were taken under ambient air atmosphere.

Scanning tunneling microscopy (STM) was performed in constant current mode on the Nanoscope IIIa / Multimode system. The tips used were made from platinum/iridium wires (80:20, diameter =

0.25 mm) cut by hand. The electrical connection between the silicon chip and the magnetic sample disk (Veeco Metrology Group, UK) was made by rubbing with In/Ga eutectic.

1.6 Raman and Luminescence Microspectroscopy

A CRM200 confocal Raman microscope (Witec GmbH, Ulm, Germany) was used to capture Raman and luminescence images and spectra. The 488 nm line of an argon ion laser or the 633 nm line of a He-Ne laser provided the excitation light and the emitted and/or scattered light passed through a Raman edge filter to remove elastically scattered light. The filtered light was collected by a multimode optical fiber which served also as the confocal pinhole. The lateral spatial resolution of the instrument is close to the diffraction limit at the given wavelength. The collected light was analysed by a spectrograph with typical settings for luminescence experiments of: 150 lines/mm (grating); an integration time of 0.1 s per pixel and 256 x 256 pixels for each image. The settings for Raman spectral imaging were: 600 lines/mm (grating); 0.5 s per pixel and 256 x 256 pixels for each image. Gold nitride films were used, rather than pure gold, as substrates for Raman spectroscopy because the morphology of these films produces a significant SERS enhancement: the preparation and characterisation of these films has been reported elsewhere.[3]

1.7 Infrared Spectroscopy

C_{11}-SiNCs were dried on an Si(100) chip and the infrared spectrum was measured in normal transmission mode. The clean Si(100) chip was used to obtain the background. The instrument was a Bio-Rad Excalibur with an MCT detector and 32 scans at 4 cm^{-1} resolution were co-added and averaged.

2 Additional Supporting Data

2.1 Optical Microscopy

Figure 2 shows optical micrographs (in reflection) of an Si(111)-C11 wafer after evaporation of C_{11}-SiNCs onto the wafer. The features that are visible are much larger than the islands[2] observed by AFM and their density on the surface is smaller: these are the large clusters referred to in the

[2]We use the term island to denote a feature composed of a single layer of nanocrystals and the term cluster to indicate features composed of multiple layers of nanocrystals.

text. An increase in the deposition time results in more such clusters, but the diameter of the largest clusters does not appear to exceed about 3 μm.

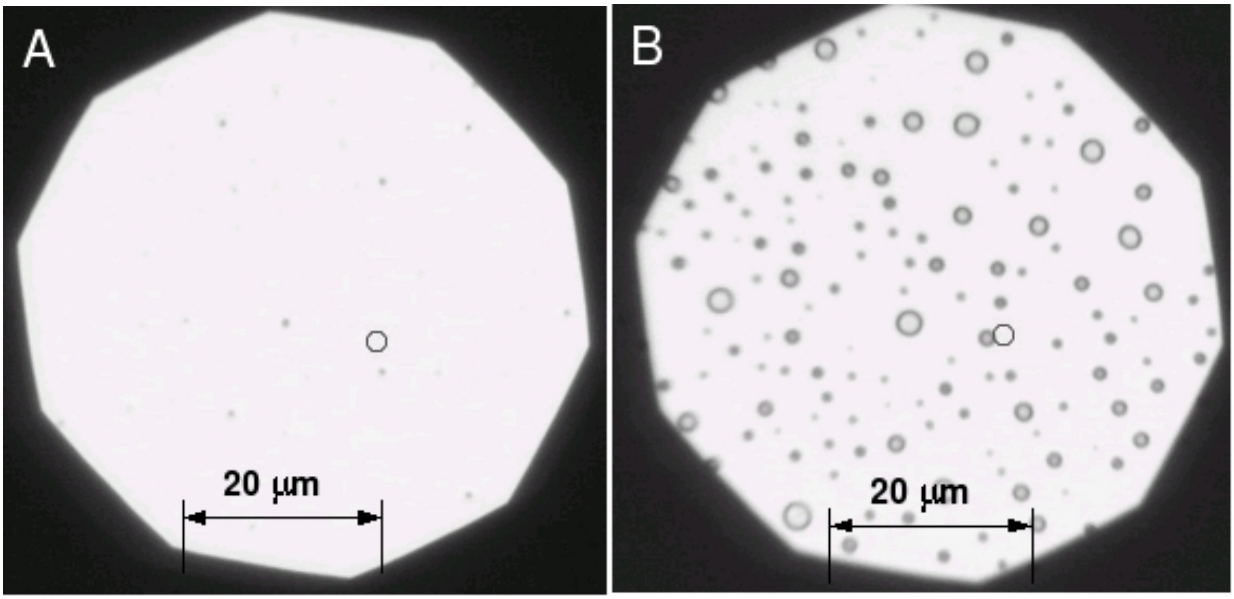

Figure 2: Optical image of C_{11}-SiNC clusters on an Si(111)-C11 wafer. (A) 15 min deposition time with the source heated at 200^0C and (B) 30 min deposition time with the source heated at 200^0C. The black circle is a marker indicating the laser focal point.

2.2 Atomic force and scanning tunneling microscopy

Figure 3 shows tapping mode AFM images of the samples shown in figure 2A. The height of the islands is ca. 5 nm and in figure 3B the underlying terrace-step morphology of the Si(111)-C11 substrate is detectable.

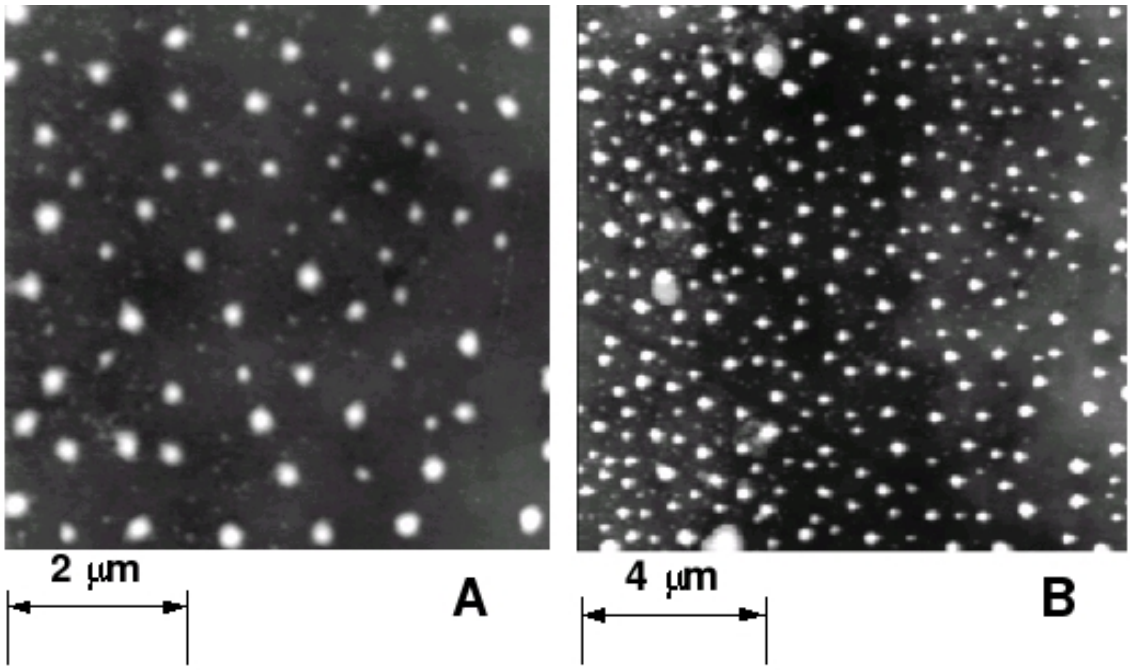

Figure 3: AFM images (tapping^{TM} mode) of C_{11}-SiNCs evaporated for 15 min onto Si(111)-C11. These images were taken on the same sample whose optical image is shown in figure 2A. In B, the terrace-step morphology of the underlying substrate is faintly visible on the left of the image as lines sloping down from left to right.

Using STM (figure 4) it was possible to resolve individual SiNCs within the islands shown in the AFM images and the mean diameter of the Si core of the particles was found to be 1.8 ± 0.34 nm.

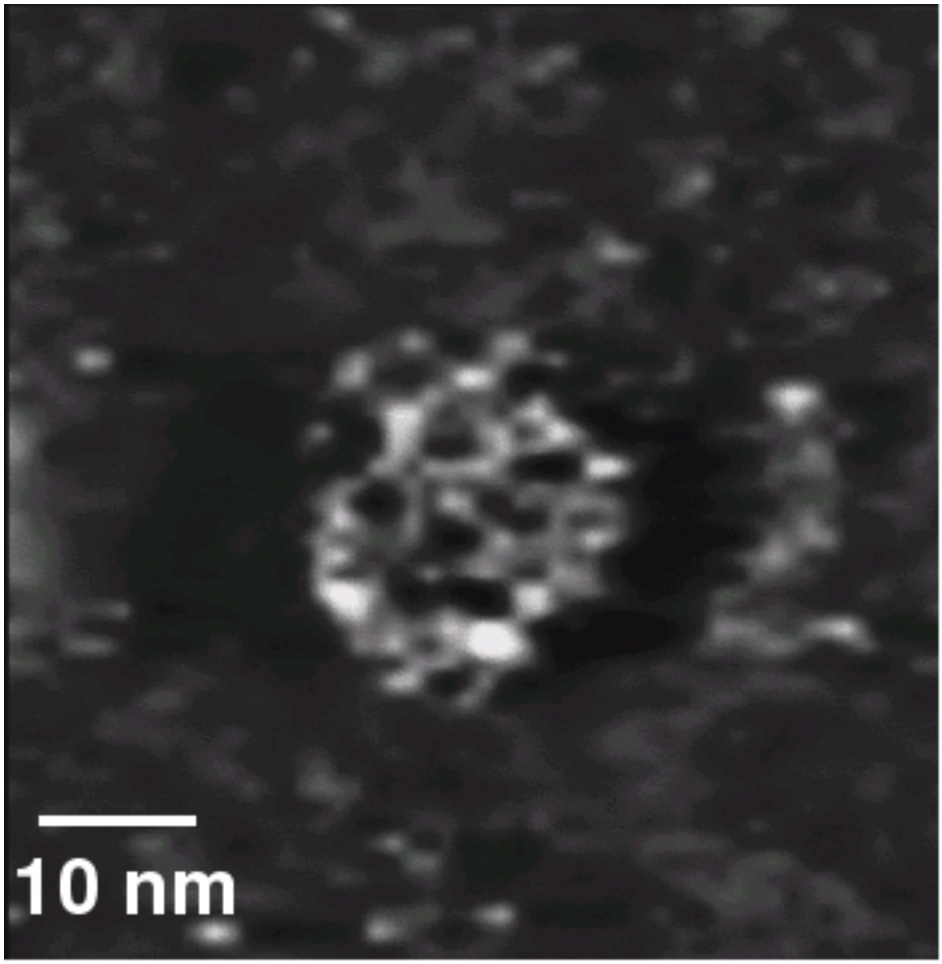

Figure 4: STM image of a single island on the sample shown in figure 3 of the main manuscript. Individual C_{11}-SiNCs are visible as white features. The bias was 1.5 V (tip vs sample) and the tunneling current was 150 pA.

2.3 Raman - Luminescence Microscopy

Figure 5 shows a luminescence image of C_{11}-SiNCs deposited on a sapphire plate by evaporation in UHV. The temperature used was 200^{o}C and was maintained for 30 min. An Ar-ion laser (488 nm) line was used to excite the luminescence and the grayscale of the image shown corresponds to the integrated emission intensity over a wavenumber range shifted 100 cm^{-1} to 6000 cm^{-1} with respect to the elastically scattered light. The diameter of the clusters of C_{11}-SiNCs (bright spots) is 1.0 ± 0.14 μm. Figure 6 is a similar luminescence image of C_{11}-SiNCs deposited on a gold nitride film showing the effect of a different substrate on the morphology of the deposit.

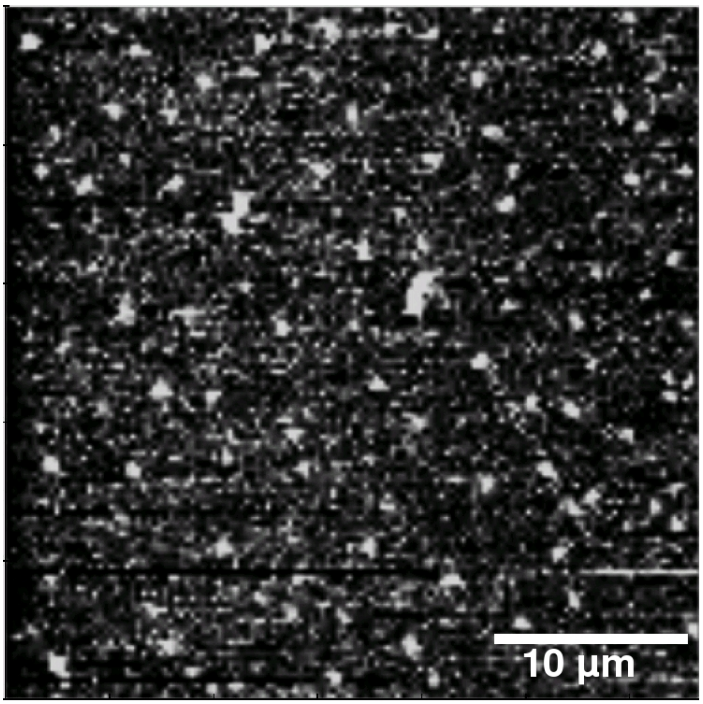

Figure 5: Confocal luminescence image of C_{11}-SiNCs deposited from the vapor on a sapphire plate (evaporation conditions: 200^{o}C for 30 min).

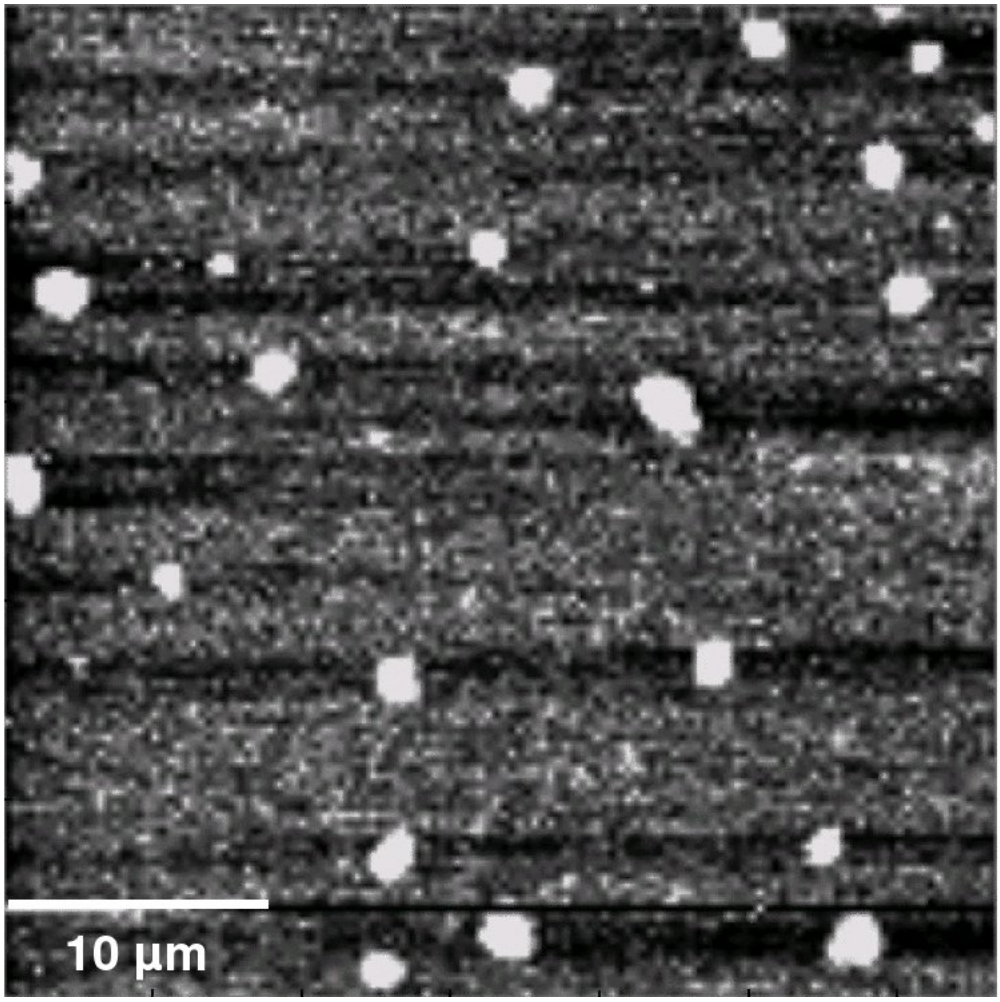

Figure 6: Confocal luminescence image of clusters (white features) of C_{11}-SiNCs deposited on a gold nitride film by evaporation in UHV. The deposition time was 30 min and the source was heated to 200^{o}C. The 488 nm line of an Argon ion laser was used to excite the sample and the backscattered (or emitted) light was collected by a multi-mode fiber, dispersed on a 150 line/mm grating and detected by a cooled CCD. The grayscale of the image corresponds to the integrated emission intensity over a wavenumber range shifted 100 cm^{-1} to 9760 cm^{-1} with respect to the elastically scattered light. The diameter of the features is 1.8 ± 0.47 μm.

Figure 7 shows a Raman image of C_{11}-SiNCs deposited on an Si(111)-C11 chip by evaporation in UHV. The temperature used was 200^{o}C and was maintained for 30 min. The light source was the 633 nm line of a He-Ne laser and the grayscale of the image shown corresponds to the scattered intensity integrated over the Raman shift range 100 cm^{-1} to 1900 cm^{-1} with respect to the elastically scattered light. The bright spots are the clusters of C_{11}-SiNCs observed in the optical image figure 2b and are sufficiently large that their Raman signal is easily discerned even on an Si substrate. The diameter of the clusters of C_{11}-SiNCs (bright spots) is 1.4 ± 0.5 μm.

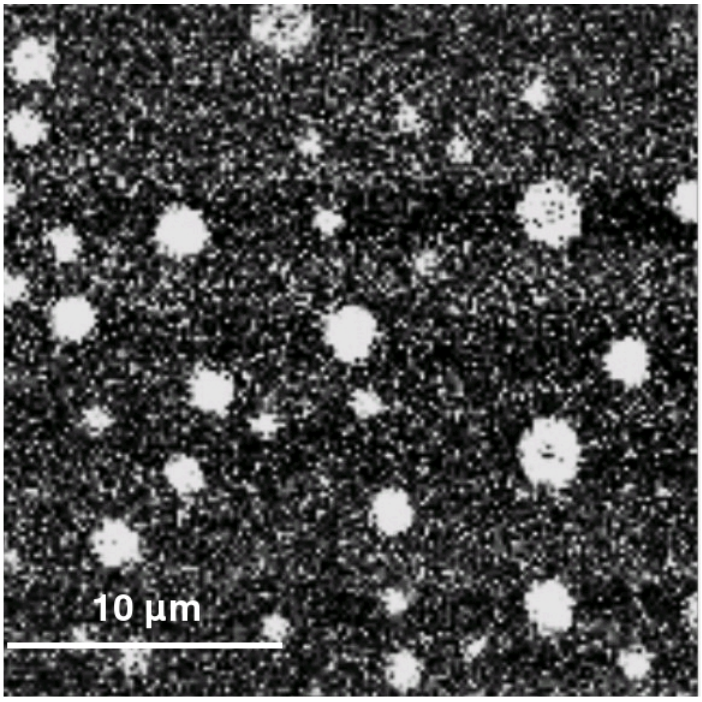

Figure 7: Confocal Raman image of C_{11}-SiNCs deposited from the vapor on an Si(111)-C11 chip (evaporation conditions: 200^{o}C for 30 min). The laser wavelength was 633 nm and the grayscale represents the scattered intensity integrated over the Stokes shift range 100 cm^{-1} to 1900 cm^{-1}. The Si phonon at ca. 520 cm^{-1} is the dominant contribution to the intensity.

2.4 X-ray Diffraction (XRD)

XRD patterns of the C_{11}-SiNCs were only obtained from films that were cast from solution, before evaporation. The amount of material deposited from the vapor was too small to obtain useful XRD data and high resolution STEM was used instead to show crystallinity (next section).

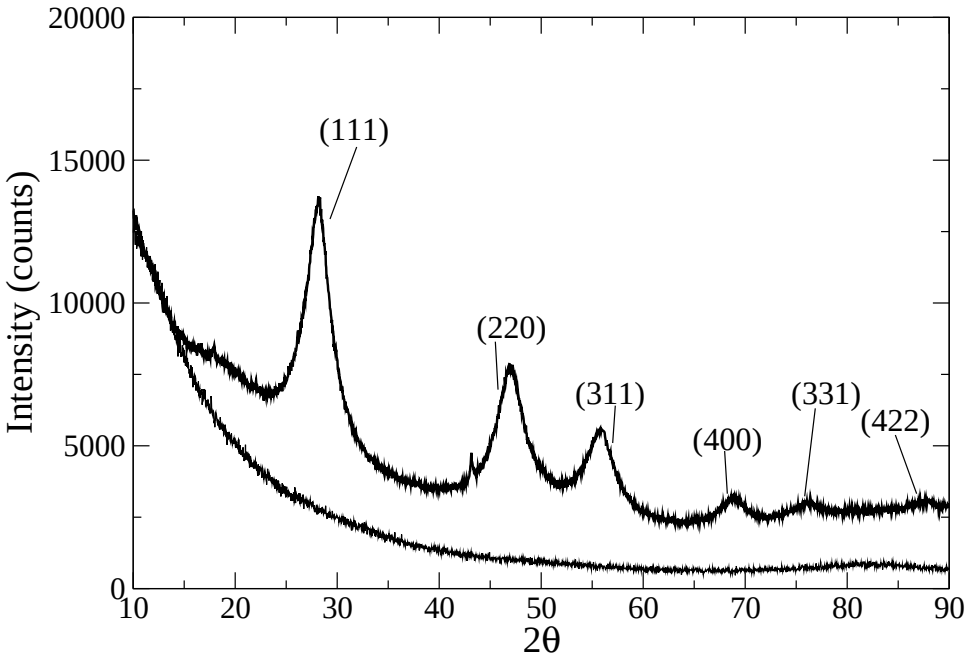

Figure 8: XRD pattern of a film of C_{11}-NCs before evaporation. The peaks are assigned to the indicated lattice planes of crystalline silicon.The lower curve is the scattering from the blank.

Table 1: Table of XRD peak positions and intensities for the C_{11}-NCs and for a bulk Si standard. [Crystalline Si Primary reference: Natl. Bur. Stand. (U.S.) Monogr. 25, 13 , 35, (1976)]

2θ Si standard	2θ C_{11}-SiNCs	Intensity (% max): Si standard	Intensity (%max): C_{11}-SiNCs
28.443	28.15	100	100
47.304	46.95	55	46
56.122	55.85	30	24
69.132	68.8	6	6
76.380	76.1	11	5
88.029	87.4	12	4

Figure 8 shows the expected peaks corresponding to crystalline silicon [3] and the data is collected in table 1. The feature at $2\theta \simeq$ 28 degrees due to (111) planes was fitted with a pseudo-Voigt function (figure 9). Using the Scherrer formula and the peak width from the fit, the Si particle diameter (assumed equal to that of the crystallite) is 2.6 nm. The value deduced from the feature at 47 degrees was the same.

[3]The small feature at 2θ =43 degrees is due to a trace of Cu on the sample stage.

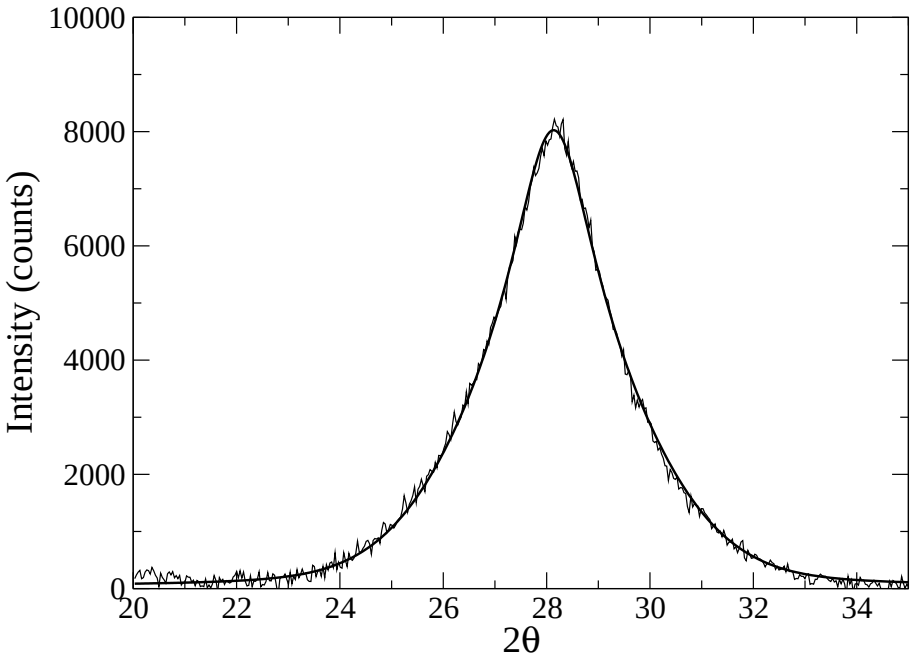

Figure 9: Pseudo-Voigt fit to the (111) peak of the XRD pattern for C_{11}-NCs after subtraction of a linear baseline.

2.5 Scanning transmission electron microscopy (STEM)

Further support for the particle size measurements and the crystallinity of the SiNCs was obtained from scanning transmission electron microscopy. The experiments were carried out in the aberration-corrected Daresbury SuperSTEM (Daresbury Laboratory, CCLRC, Daresbury, UK). High resolution bright field and high angle annular dark field (HAADF) images, the latter revealing atomic Z-contrast, were taken simultaneously.

Figure 10 shows a typical high resolution STEM HAADF (aberration-corrected) image of a single C_{11}-SiNC on a carbon grid. The sample was prepared by placing a drop of dichloromethane solution of C_{11}-SiNCs on a standard carbon grid. The particle is roughly spherical and the diameter is about 2.5 nm. Electron energy loss spectra (Si L edge) showed that the white area in the image corresponds to the Si core and not the alkyl capping monolayer (figure 11). The EEL spectra (Si L edge) for all SiNCs, including evaporated material were similar. A detailed study will be published elsewhere.

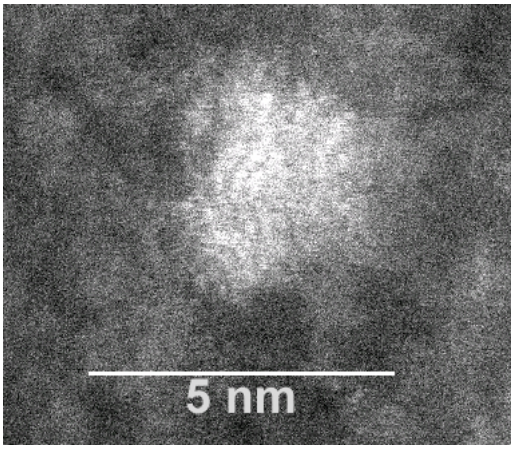

Figure 10: STEM HAADF (aberration-corrected) image of a single C_{11}-SiNC particle cast from dichloromethane solution onto a carbon grid. The white region corresponds to the Si core. The beam energy was 100 keV and the resolution was about 0.1 nm.

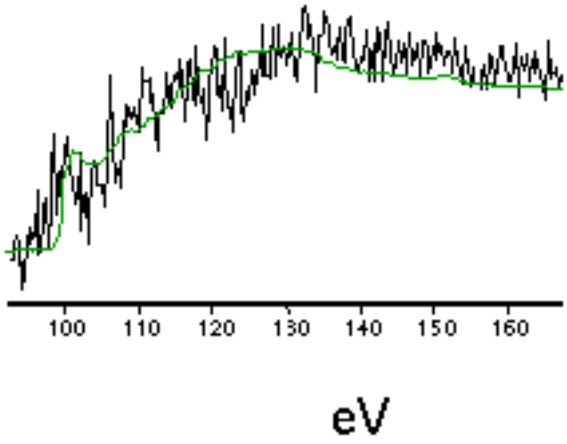

Figure 11: Electron energy loss spectrum (Si L edge) from the centre of the particle shown in figure 10. The Si reference spectrum is overlaid as a green line.

We also obtained high resolution STEM images of the C_{11}-SiNCs that were evaporated at 200^0C and deposited on a carbon grid placed in the UHV chamber as the receiving substrate. The presence of Si was confirmed by electron energy loss spectra (Si L edge) and the direct observation of lattice fringes of the appropriate spacing. The particles tend to cluster on the grid and figure 12 shows (in HAADF) the same cluster of C_{11}-SiNCs presented in the main text (in bright field), though the focus is slightly different. In both cases, the image quality is slightly better than for the material deposited from solution; this is probably due to the removal of trace solvent (known to affect imaging of SiNCs [4]) as the UHV chamber is pumped down.

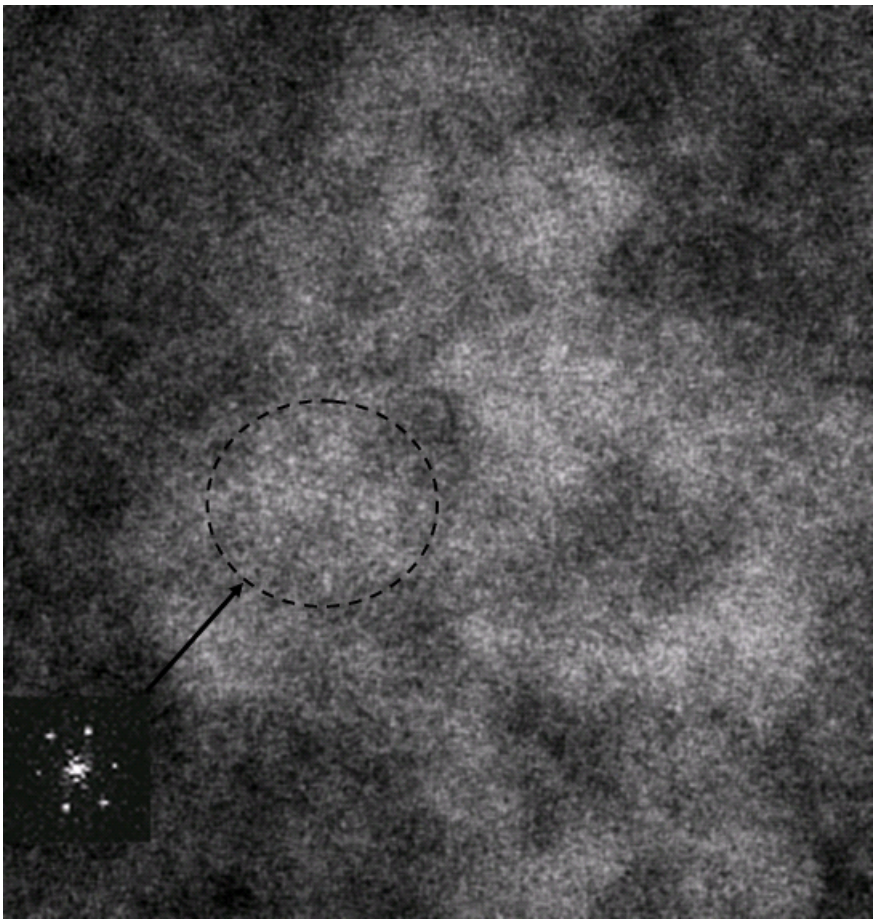

Figure 12: STEM HAADF (aberration-corrected) image of C_{11}SiNCs evapoarted (at 200^0C) onto a carbon grid. The white features are the Si cores of the NCs and the surrounding 'halo' is probably due to the undecyl chains bonded to the Si. The beam energy was 100 keV and the resolution was about 0.1 nm. The inset shows the Fourier transformed image of the circled particle which matches closely to that expected for the (111) lattice planes of crystalline Si.

Figure 13 shows another example, typical, of a cluster of C_{11}-SiNCs, the lattice fringes of individual NCs are still, however, visible.

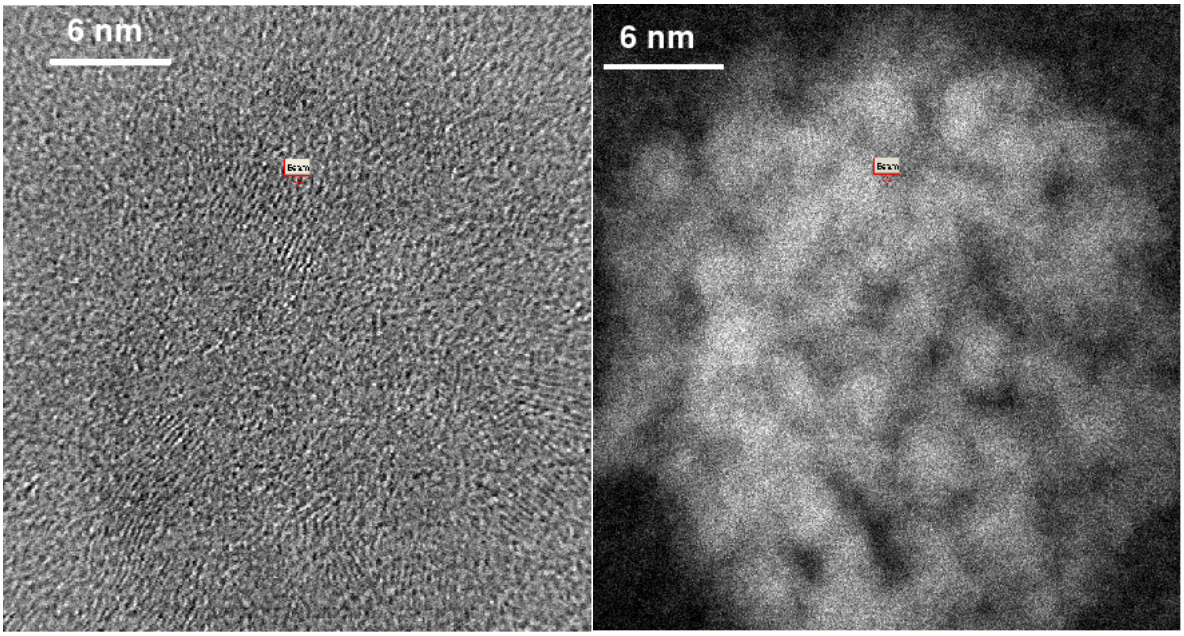

Figure 13: Left: Bright field and Right: HAADF images of a cluster of C_{11}-NCs deposited from the vapor on a carbon grid. The evaporation temperature was 200^0C.

Two additional STEM images (bright field and HAADF) of an isolated particle (less common than the clusters) are shown in figure 14. The Si(111) lattice is particularly clear in this example (inside circled regions), but the halo which is likely to be due to the surrounding undecyl chains is still visible.

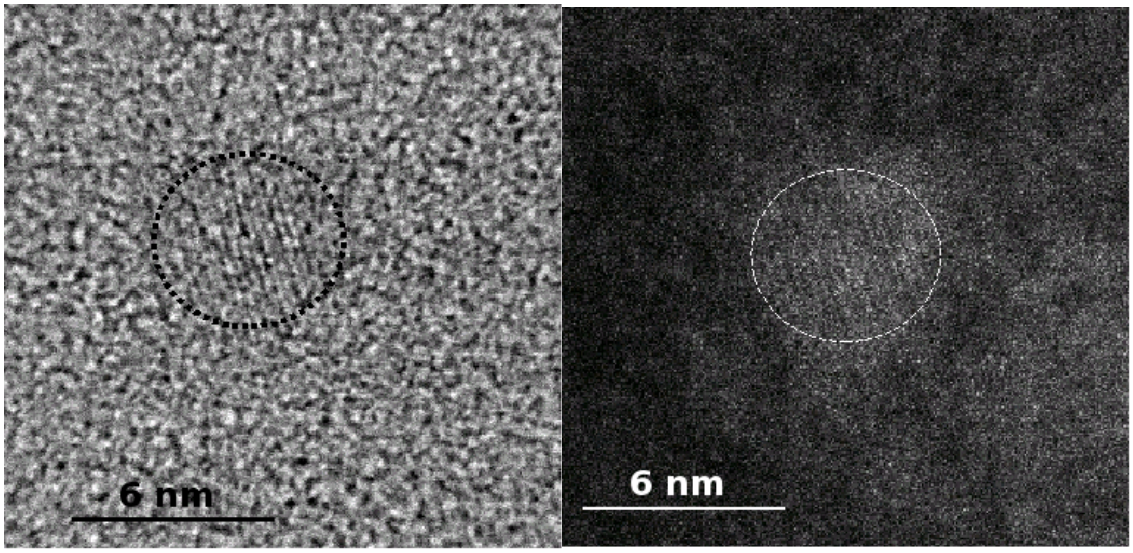

Figure 14: Bright field and high angle annular dark field (HAADF) image of an isolated particle. Even though this NC is not part of an aggregate, a halo surrounding the crystalline Si core can be seen here too. The Si(111) lattice planes are strongly visible. The evaporation temperature was 200^0C.

2.6 Small angle x-ray scattering - particle sizing

SAXS measurements were performed at synchrotron beamline 2.1 (CCLRC, Daresbury, UK) with a fixed x-ray wavelength of 0.154 nm. The x-rays were focused in both horizontal and vertical directions by means of a triangular monochromator and a plane mirror. The camera length was 4.5 m. The Guinier approximation was fitted to the scattering data for samples of C_{11}-SiNCs dispersed in toluene (figure 15) to extract the particle size (Si core diameter = 2.4 nm).[5] In view of the weak scattering by Si, the curved region at low Q is likely due to a miscancellation after subtraction of the scattering of the solvent, though we cannot rule out form-factor scattering due to particle aggregates.

The particle diameter obtained from these experiments was interpreted as that of the silicon core on two grounds: (i) the background from the solvent, which is a hydrocarbon with a similar scattering factor to the alkyl monolayer on the particles, was subtracted from the scattering profile before analysis and (ii) the diameter obtained for particles prepared with C6 (hexyl) and C11 (undecyl) monolayers was the same within experimental error.

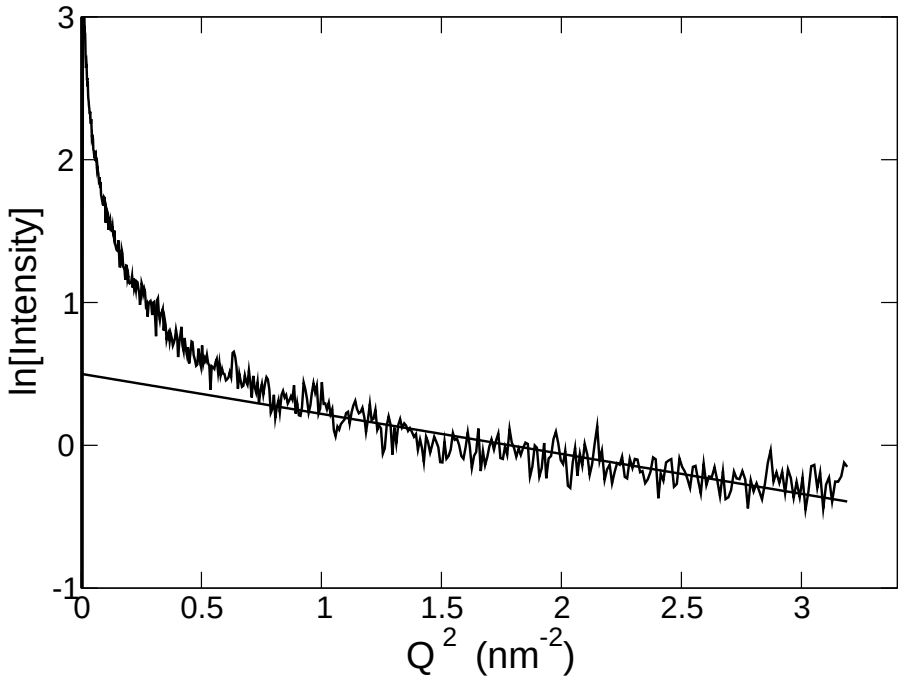

Figure 15: Guinier plot for C_{11}-SiNCs dispersed in toluene.

2.7 Infrared spectroscopy

Figure 16 shows an infrared spectrum of the as-prepared C_{11}-SiNCs. This spectrum shows the same features as our previously published data,[1] but the signal-to-noise ratio is better because we have now been able to prepare larger samples. The following features are worth noting: (1) the absence of vinylic C-H stretches above 3000 cm^{-1} and the absence of the sharp C=C stretch at 1640 cm^{-1} indicates the sp^2 carbons have rehybridised to sp^3; (2) aliphatic C-H stretches in the range 2960 - 2850 cm^{-1} and the methylene scissor mode at ca. 1470 $cm^{-1}$are characteristic of an n-alkyl layer; (3) the broadened Si-H stretching feature at ca 2100 cm^{-1} is characteristic of residual Si-H on alkylated silicon [6] and (4) the broad feature at ca. 1050 cm^{-1} confirms the presence of a small amount of silicon oxide in agreement with the photoemission data. The coverage of oxide is less than that of alkyl chains based on the relative intensities of the features due to Si-O and C-H vibrations as well as the absence of a distinct feature at 2250 cm^{-1} due to Si-H stretches in which the Si atom is backbonded to three oxygen atoms.

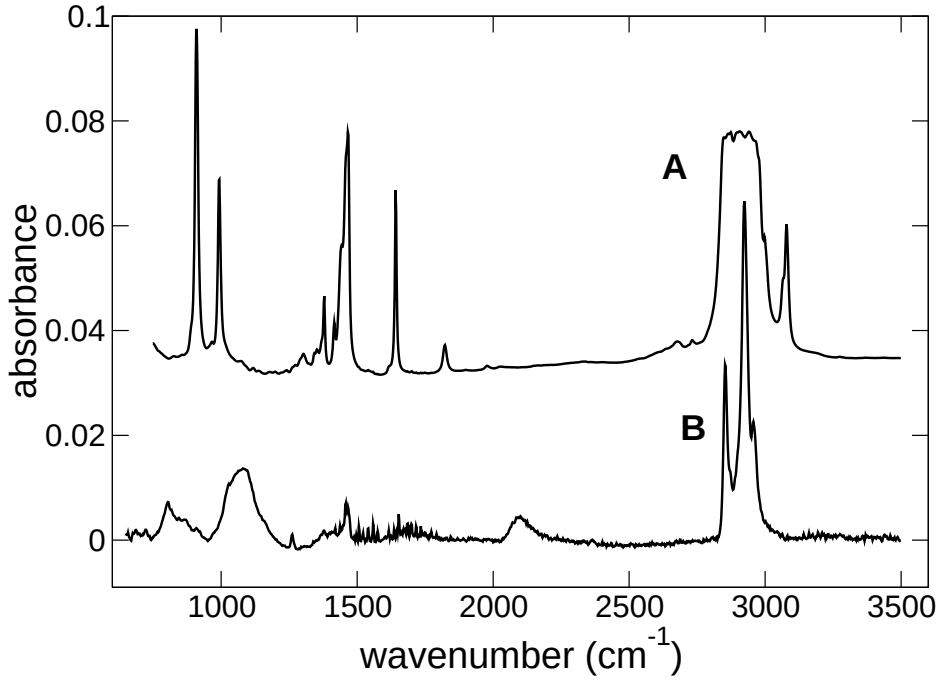

Figure 16: FTIR spectra in normal transmission of (A) a drop of undec-1-ene and (B) C_{11}-SiNCs deposited from solution, on a 1 cm^2 Si(100) chip. In both cases the background was the same chip before deposition of the undecene or alkyl-SiNCs: it should be noted that Si-H stretches are not observable in normal transmission on such a chip.

References

[1] Lie, L.H.et al. Immobilisation and synthesis of DNA on Si(111), nanocrystalline porous silicon and silicon nanoparticles. *Faraday Discuss.* **125**, 235-249 (2004).

[2] Lie, L.H., Duerdin,M., Tuite, E.M., Houlton, A., and Horrocks, B.R. Preparation and characterisation of luminescent alkylated silicon quantum dots. *J. Electroanal. Chem.* **538**, 183-190 (2002).

[3] Šiller, L. et al. Gold film with gold nitride - a conductor but harder than gold. Appl. Phys. Lett. 86, 221912 (2005).

[4] Li, X. G., He, Y. Q., and Swihart, M. T. Surface functionalization of silicon nanoparticles produced by laser-driven pyrolysis of silane followed by HF-HNO_3 etching. *Langmuir* **20**, 4720-4727 (2004).

[5] Guinier, A. *Nature* (*London*) **142**, 569 (1938).

[6] de Smet, L. C. P. M. et al. Mechanism of the hydrosilylation reaction of alkenes at porous silicon: experimental and computational deuterium labelling studies. *J. Phys. Chem. B* **109**, 12020-12031 (2005).